NASA TM-84477

NASA Technical Memorandum 84477

NASA-TM-84477 19820017494

THE EFFECT OF WATER VAPOR ON FATIGUE CRACK GROWTH IN 7475-T651 ALUMINUM ALLOY PLATE

DENNIS L. DICUS

MAY 1982

National Aeronautics and Space Administration

Langley Research Center
Hampton, Virginia 23665

ABSTRACT

An investigation was performed to assess the effects of water vapor on fatigue crack growth in 7475-T651 aluminum alloy plate at frequencies of 1 Hz and 10 Hz. Twenty-five mm thick compact specimens were subjected to constant amplitude fatigue testing at a load ratio of 0.2. Fatigue crack growth rates were calculated from effective crack lengths determined using a compliance method. Tests were conducted in hard vacuum and at water vapor partial pressures ranging from 94 Pa to 3.8 kPa.

Fatigue crack growth rates were frequency-insensitive under all environmental conditions tested. For constant stress intensity factor ranges crack growth rate transitions occurred at low and high water vapor pressures. Crack growth rates at intermediate pressures were relatively constant and showed reasonable agreement with published data for two Al-Cu-Mg alloys. The existence of two crack growth rate transitions suggests either a change in rate controlling kinetics or a change in corrosion fatigue mechanism as a function of water vapor pressure. Reduced residual deformation and transverse cracking on specimens tested in water vapor versus vacuum may be evidence of embrittlement within the plastic zone due to environmental interaction.

INTRODUCTION

Corrosion-fatigue, the response of a material to the combined actions of cyclic stress and a corrosive environment, is recognized as a principal factor in accelerating structural degradation of aerospace vehicles in service. A lack of understanding of the fundamental mechanisms involved in chemical/mechanical environment interactions has seriously limited consideration of corrosion fatigue in the structural design process and in alloy development.

The susceptibility of aluminum alloys, the most widely used materials of aircraft construction, to corrosion fatigue in even relatively innocuous environments such as air is well known. There is general agreement in the literature that water vapor has a much greater effect on fatigue in aluminum alloys than the other constituents of pure air. Dry nitrogen appears to have no detrimental effect [1,2], and except in nearly pure aluminum, dry oxygen appears to have little if any effect on the fatigue of aluminum alloys [2-5]. On the other hand, wet nitrogen, wet oxygen, wet air, and pure water vapor shorten fatigue lives and accelerate fatigue crack growth rates of aluminum alloys [1-8]. The severity of the effect is a function of the water vapor pressure [2-4, 6-8], and no effect occurs below some water vapor pressure threshold [2-8].

The present study was undertaken to assess the effects of water vapor on fatigue crack growth in 7475-T651 aluminum alloy plate at frequencies of interest for aerospace applications. Because of its excellent balance of tensile properties, fracture toughness, and fatigue resistance, 7475 (an improved chemistry modification of the widely used 7075 alloy) is expected to find increased application in future aerospace vehicles. Fatigue crack growth rates were determined at frequencies of 1 Hz and 10 Hz in hard vacuum and in mixtures of water vapor and nitrogen at various partial pressures of water vapor. Fracture surfaces were characterized in an attempt to correlate fracture morphology with environmental interaction.

SYMBOLS

a	crack length, m
b_j	coefficients in compliance calibration equation
B	thickness of compact specimen, m (See Fig. 1.)
da/dN	fatigue crack growth rate, m/cycle
E	modulus of elasticity, Pa
H	half height of compact specimen, m (See Fig. 1.)
i,j	indices
K	stress intensity factor, $N/m^{3/2}$
ΔK	stress intensity factor range in fatigue cycle, $N/m^{3/2}$
N	number of load cycles
P	applied load, N
ΔP	load range in fatigue cycle, N
R	ratio of minimum load to maximum load
V	crack-opening displacement at the crack mouth of compact specimen, m
ΔV	crack-opening displacement range in fatigue cycle, m
W	width of compact specimen, m (See Fig. 1.)

EXPERIMENTAL DETAILS

The material used in this study was aluminum alloy 7475-T651; the chemical composition, as reported by the manufacturer, is shown in Table 1. All specimens were cut from a single 25.4 mm thick plate of the alloy. The tensile and fracture properties of the plate are shown in Table 2. Standard compact (CT) specimens with a straight-through notch and integral knife edges at the notch mouth were machined from the plate. The specimen configuration is shown in Fig. 1. Specimen thickness, B, was nominally 25 mm, and initial uncracked a/W ratios ranged from 0.45 to 0.50.

Fatigue crack growth experiments were performed in an environmental fatigue testing system capable of maintaining either vacuum or controlled gaseous environments. Basically the system consisted of an environmental chamber mounted on a servocontrolled, closed-loop, hydraulically-actuated testing machine. Details of this system are given in Refs 9 and 10.

Experiments were performed at ambient temperature in a vacuum of 130 μPa to obtain fatigue crack growth rates in an inert, reference environment and in mixtures of water vapor and nitrogen at water vapor partial pressures ranging from 94 Pa to 3.8 kPa. For vacuum tests the chamber was initially evacuated to a pressure of 70 μPa. The pressure was then adjusted and maintained at 130 μPa by an automatic pressure control unit which admitted appropriate quantities of air while the chamber was continuously pumped. For the water vapor-nitrogen experiments, the chamber was initially evacuated to a pressure of 130 μPa or less and was backfilled with a water vapor-nitrogen mixture immediately after stopping the pumps. The water vapor-nitrogen mixtures were obtained by bubbling high purity nitrogen gas through a heated column of distilled water.

Nitrogen was chosen as the carrier gas because it is inert with respect to aluminum. Conditions within the chamber were allowed to stabilize for approximately one hour before beginning a fatigue experiment. Total pressure, dew point, and dry bulb temperature within the chamber were monitored continuously by an electronic manometer, a hygrometer, and a copper-constantan thermocouple, respectively. In most tests water vapor pressure varied ±2 percent or less, but in tests at nominal pressures of 2.62 kPa and 150 Pa, water vapor pressure varied ±6 percent and ±15 percent, respectively.

Experiments were performed under constant amplitude loading with R = 0.2 under load control at frequencies of 1 Hz and 10 Hz using a sinusoidal waveform. Maximum and minimum loads for all tests in water vapor-nitrogen mixtures were set to produce an initial stress intensity factor range of 8.8 $MN/m^{3/2}$. Tests in vacuum employed initial stress intensity factor ranges of 8.8 $MN/m^{3/2}$ or 17.6 $MN/m^{3/2}$. Prior to carrying out tests in controlled environments, specimens were fatigued in laboratory air to extend a starter crack about 1.3 mm from the notch tip. Tests in controlled environments were performed without interruption to avoid transient effects on crack growth rate. To preclude notch geometry effects crack growth rates were not calculated until a crack had extended at least 3 mm from the notch tip.

Effective crack lengths were determined continuously during fatigue testing by a compliance method. The crack-opening displacement at the notch mouth, V, was monitored by a clip gage mounted on the specimens integral knife edges. The clip gage and load cell signals were fed to peak-reading digital voltmeters for determination of the maximum and minimum displacements and loads occurring

during fatigue cycling. Values of the effective crack length were calculated from the compliance calibration equation

$$a/W = \sum_{j=0}^{3} b_j [\ln(EBV/P)]^j = \sum_{j=0}^{3} b_j [\ln(EB\Delta V/\Delta P)]^j \qquad (1)$$

where $b_0 = -1.0429$, $b_1 = 0.5609$, $b_2 = -0.0470$, and $b_3 = 0.0008$, and E was determined experimentally for the material. Eq 1 is based on a theoretical calculation of compliance of the CT specimen configuration by Newman [11] and was developed using regression analysis employing the method of least squares. A comparison between Eq 1 and Newman's theoretically calculated values is shown in Fig. 2. Values of a/W computed using Eq 1 are within ±0.4 percent of the theoretical values for $0.2 \leq a/W \leq 0.8$. For additional details concerning the development of Eq 1, see Ref 9.

Fatigue crack growth rates were calculated by averaging the secants between three sequential a,N data points. For the ith data point

$$da/dN = \frac{\dfrac{a_i - a_{i-1}}{N_i - N_{i-1}} + \dfrac{a_{i+1} - a_i}{N_{i+1} - N_i}}{2}$$

Of course, da/dN was not calculated for either the first or last crack lengths.

Stress intensity factors were calculated using the expression for the CT specimen configuration from ASTM Method for Plain-Strain Fracture Toughness Testing of Metallic Materials (E399-78a)

$$K = \frac{P}{BW^{1/2}} \left[\frac{2 + \frac{a}{W}}{(1 - \frac{a}{W})^{3/2}}\right] \left[0.866 + 4.64 \frac{a}{W} - 13.32 \frac{a^2}{W^2} + 14.72 \frac{a^3}{W^3} - 5.6 \frac{a^4}{W^4}\right]$$

Fracture surface morphology was characterized optically and by scanning electron microscopy. Immediately after broken specimens were removed from the environmental fatigue testing system, fracture surfaces were sprayed with a clear acrylic lacquer to prevent contamination. The lacquer was removed prior to microscopic examination by cleaning in acetone.

RESULTS AND DISCUSSION

Fatigue Crack Growth Behavior

Fig. 3 shows fatigue crack growth rate as a function of ΔK for the LT orientation in hard vacuum at frequencies of 1 Hz and 10 Hz. These results clearly indicate the absence of a frequency effect on fatigue crack growth rates in an inert environment. Results obtained for the TL orientation (not shown) in hard vacuum also displayed no discernable difference in fatigue crack growth rates at these frequencies. Fatigue crack growth rates for the two orientations were nearly identical at low ΔK values, and little difference in crack growth rates was observed except at ΔK values in excess of 20 $MN/m^{3/2}$ where crack growth rates for TL orientation were somewhat higher than those for the LT orientation. For experiments in water vapor-nitrogen mixtures, only the LT orientation was used.

Fig. 4 shows fatigue crack growth rate as a function of ΔK for various water vapor pressures and in vacuum at a frequency of 1 Hz. These water vapor pressures range from 94 Pa to 3.8 kPa and correspond to relative humidities ranging from about 4 percent at 22°C to about 100 percent at 28°C. At low ΔK values crack growth rates at the lowest and highest water vapor pressures were, respectively, about two times higher and five times higher than crack growth rates in vacuum. Similar fatigue crack growth response was observed for water

vapor pressures from 94 Pa to 1.03 kPa, but the effect of water vapor on crack growth rates was significantly greater for pressures from 2.61 to 3.8 kPa. At high ΔK values crack growth rates at water vapor pressures of 1.03 kPa and less tended to converge with rates in vacuum, but crack growth rates at the higher water vapor pressures remained substantially higher than the rates in vacuum. Fig. 5 shows data obtained under similar environmental conditions at a frequency of 10 Hz. A comparison of Figs. 4 and 5 indicates that the general trends in the fatigue crack growth behavior at 10 Hz were similar to the trends observed at 1 Hz. At the same values of ΔK, the effect of frequency on fatigue crack growth rates at similar values of water vapor pressure was insignificant.

The variation of fatigue crack growth rate with water vapor pressure at four ΔK levels is shown in Fig. 6. Since the predominant component of the residual gas in a vacuum of 130 μPa is water vapor, the crack growth data obtained in hard vacuum are plotted as if the total pressure were due to water vapor only. This figure shows data from both the 1 Hz and 10 Hz tests and clearly indicates the relative insensitivity of the fatigue crack growth response to frequency at all water vapor pressures tested. The effect of water vapor on fatigue crack growth rates was qualitatively similar at each ΔK level. Even at the lowest water vapor pressure used in these tests (94 Pa), a relatively dry condition, a significant effect of water vapor on crack growth rates was apparent. Little change in the crack growth rates occurred over the water vapor pressure range from 94 Pa to 1.03 kPa. However, an abrupt acceleration in crack growth rates was observed at higher water vapor pressures. Two transitions in crack growth rates as a function of water vapor pressure are indicated by these results. The first transition occurred somewhere between hard vacuum levels and 94 Pa, and the second transition occurred at pressures in excess of 1.03 kPa.

These results also indicate that corrosion fatigue of 7475-T851 in water vapor is not due to a simple interaction (superposition) of mechanical fatigue and stress corrosion cracking but is more likely the result of a more complex phenomenon. Although fatigue crack growth rates were as much as five times higher in water vapor than in hard vacuum, crack growth rates in water vapor were unaffected by a ten fold change in frequency. If the acceleration of fatigue crack growth rates in water vapor were a result of stress corrosion cracking, fatigue crack growth rates should have been higher at 1 Hz than 10 Hz. Of course, this does not preclude some contribution of stress corrosion cracking to the corrosion fatigue of 7475-T651 in water vapor at frequencies less than 1 Hz.

Wei et al. [8] studied the effect of water vapor on fatigue crack growth in 16.5 mm thick specimens of the Al-Cu-Mg alloy 2219-T851 at a frequency of 5 Hz. The present results for 7475-T651, an Al-Zn-Mg-Cu alloy, are compared to the results for 2219-T851 at a ΔK value of 15 $MN/m^{3/2}$ in Fig. 7. For 2219-T851 fatigue crack growth rates were virtually unaffected by water vapor until a threshold pressure was reached. Crack growth rates then increased rapidly but reached a maximum value at a water vapor pressure only one order of magnitude higher than the threshold pressure. The present results for 7475-T651 show good agreement with Wei's data for 2219-T851 at hard vacuum conditions and at water vapor pressures over the range from 94 Pa to 1.03 kPa. The similarity of crack growth rates for the two alloys in both vacuum and water vapor suggests a common corrosion fatigue mechanism for Al-Cu-Mg and Al-Zn-Mg-Cu alloys and supports the contention that stress corrosion cracking plays little role in corrosion fatigue of aluminum alloys in water vapor.

Bradshaw and Wheeler [2] studied the effect of water vapor on fatigue crack growth in 1.6 mm thick specimens of the Al-Cu-Mg alloy DTD 5070A at frequencies of 1 Hz and 100 Hz. The present results for 7475-T651 are compared to the results for DTD 5070A at a ΔK value of 12 $MN/m^{3/2}$ in Fig. 8. Similar to the results for 2219-T851 (Fig. 7), the results for DTD 5070A display a threshold water vapor pressure below which crack growth rates were unaffected by water vapor and a relatively narrow pressure region over which a rapid transition in crack growth rates occurred. For DTD 5070A the transition in crack growth rates was frequency sensitive; a 100 fold increase in the frequency produced two orders of magnitude increase in the threshold water vapor pressure. The present results for 7475-T651 show good agreement with Bradshaw and Wheeler's data for DTD 5070A at hard vacuum conditions and at intermediate water vapor pressures (94 Pa to 1.03 kPa) once transition was complete. Although the present results for 7475-T651 indicate the existence of a crack growth rate transition at water vapor pressures less than 94 Pa, a second frequency-insensitive crack growth rate transition was observed at very high water vapor pressures. This second crack growth rate transition for 7475-T651 occurred at water vapor pressures in excess of the highest pressures at which 2219-T851 and DTD 5070A were tested.

Fractographic Characterization

Fracture surfaces of specimens fatigued in hard vacuum and at various water vapor pressures were characterized in an attempt to correlate fracture morphology with environmental interaction. Macroscopically, the fracture morphology of specimens tested in vacuum contrasted sharply with that of specimens tested in water vapor. As illustrated in Fig. 9, the fracture morphology of specimens tested in vacuum varied across the thickness of the

specimens. Compared to the mid-thickness region, the fracture surface near the edges was highly roughened or rumpled, having an undulated appearance. The roughened portions of the fracture surface appeared to have grown toward the center of the specimen with increasing ΔK. This change in morphology from the center to the edges indicates a change in fatigue crack propagation mode associated with a change of stress state along the crack front. In the mid-thickness region where the fracture plane was normal to the applied load axis, the crack propagated predominantly in the opening (tensile) mode. However, the highly roughened surface indicates that the crack propagated in a mixed opening/sliding (tensile/shear) mode in the near-edge regions.

Fig. 10 shows optical macrographs of specimens tested at low and high water vapor pressures. Compared to specimens tested in vacuum, these specimens exhibited a more uniform fracture morphology across the thicknesss. Although some roughening of the near-edge regions was exhibited by specimens tested at low water vapor pressure (Fig. 10(a)), the process began at higher ΔK values and involved much less of the fracture surface than for specimens tested in vacuum. Little evidence of fracture surface roughening was found on specimens tested at high water vapor pressures (Fig. 10(b)), but crack front curvature was noticeable at high ΔK values near the onset of fast fracture.

Differences in the amount of residual deformation on the fracture surfaces of specimens tested in water vapor and vacuum may be evidence of environmental interaction within the plastic zone ahead of the crack tip. Reduced residual deformation on the fracture surfaces of specimens tested in water vapor may be the result of embrittlement within the plastic zone.

The apparent differences in residual deformation and crack propagation mode in the near-edge regions may account for differences in fatigue crack growth rates in vacuum and water vapor. Greater residual deformation may have

caused crack closure at higher loads in vacuum than water vapor, and mixed mode crack propagation near the edges may have retarded the overall fatigue crack growth rate in vacuum.

The marked contrast in macroscopic fracture appearance for specimens tested in vacuum and water vapor was not evident microscopically. At relatively low magnification in the scanning electron microscope, the fracture morphology of specimens tested at all water vapor pressures was generally similar to that of specimens tested in vacuum for similar ΔK values. No significant difference in morphology for near-edge and mid-thickness regions was detected regardless of the test environment.

Fatigue striations were found on the fracture surfaces of specimens tested in vacuum and water vapor. However, the appearance of striations formed in vacuum and water vapor was quite different, and striations were much less prevalent on specimens tested in vacuum. Fatigue striations formed in water vapor (Fig. 11(a)) were classic in appearance, but striations formed in vacuum (Fig. 11(b)) were poorly defined and exhibited large, local variations in spacing. Measured striation spacings were compared to fatigue crack growth rates. In general, good agreement was found for specimens tested in water vapor, but large discrepencies were found for specimens tested in vacuum.

In addition to fatigue striations, numerous areas of transverse cracking were found at low to moderate ΔK values on specimens tested in vacuum. Examples are shown in Fig. 12. These transverse cracks were parallel and fairly regularly spaced. Fine striation-like markings were found on the relatively flat surfaces between the cracks. Although some transverse cracks were also found on specimens tested in water vapor, this feature was much more prevalent on specimens tested in vacuum. The much lower amount of transverse cracking exhibited by specimens tested in water vapor may be additional evidence of localized embrittlement within the plastic zone.

Mechanisms

The enhancement of aluminum alloy fatigue crack growth rates by water vapor has been attributed to hydrogen embrittlement [1,3,5,8]. Such a mechanism involves a series of sequential or concurrent steps or processes which have been described by Marcus [12] for the general case of gas-metal interactions during fatigue. Following the diffusional transport of water vapor to the crack tip vicinity, molecular water is adsorbed on the clean aluminum surface produced by the advancing crack. The reaction of water with aluminum produces an oxide or hydrated oxide film and liberates hydrogen. After dissociation to the atomic or ionic form, hydrogen adsorbs on the aluminum surface, enters the aluminum lattice, and is transported into the plastic zone ahead of the crack tip where localized embrittlement occurs. In addition to normal bulk diffusion, hydrogen transport within the plastic zone is presumed to occur by pipe diffusion through the dense dislocation network at the crack tip and mobile dislocation sweep-in [13].

If hydrogen embrittlement is the causative mechanism, fatigue crack growth rates in water vapor would depend on the kinetics associated with the processes outlined above. The rate controlling process may be the transport of water vapor to the crack tip vicinity, the reaction of water and aluminum to produce atomic or ionic hydrogen, or the rate of diffusion of hydrogen within the plastic zone ahead of the crack tip. The present results for 7475-T651 and those of Bradshaw and Wheeler [2] and Wei et al. [8] for the Al-Cu-Mg alloys DTD 5070A and 2219-T851 showed a crack growth rate transition that occurred at relatively low water vapor pressures. Mathematical models [14] have been developed for the limiting cases of gas phase transport control and surface reaction

rate control with the assumption that these processes are slower than hydrogen diffusion within the plastic zone. Predictions from the gas phase transport control model have shown reasonable correlation [8,15] with the data for DTD 5070A and 2219-T851. These correlations support the suggestion of Bradshaw and Wheeler [2] that corrosion fatigue crack growth rates for aluminum alloys in water vapor are related to the exposure (pressure X time) during each load cycle.

Although the present results for 7475-T651 indicate a crack growth rate transition at low water vapor pressures, a second, frequency-insensitive crack growth rate transition was observed at high water vapor pressures. If both of these crack growth rate transitions are due to hydrogen embrittlement, either the rate controlling process or the specific embrittlement mechanism must change as a function of pressure. Alternatively, the transition at high pressure may be due to some other mechanism acting in concert with or instead of hydrogen embrittlement. Although the fractographic evidence presented herein tends to support plastic zone embrittlement, anodic reactions in the crack tip region must necessarily accompany the cathodic reactions that produce hydrogen. Since the relative humidity levels during the tests at high water vapor pressure were at or near 100 percent, water reaching the crack tip may have been liquid rather than vapor. A bulk liquid phase at the crack tip may be favorable for the onset of an anodic dissolution mechanism.

CONCLUSIONS

An investigation has been performed to assess the effects of water vapor on fatigue crack growth in 7475-T651 aluminum alloy plate at frequencies of

interest for aerospace applications. Fatigue crack growth rates were determined at frequencies of 1 Hz and 10 Hz in hard vacuum and in mixtures of water vapor and nitrogen at water vapor partial pressures ranging from 94 Pa to 3.8 kPa. The important findings and conclusions from this study are as follows:

1. Two crack growth rate transitions were observed as a function of water vapor pressure for constant stress intensity factor ranges. One transition occurred at water vapor pressures less than 94 Pa, and the second transition occurred at pressures in excess of 1.03 kPa. At intermediate water vapor pressures and at hard vacuum, the present results show reasonable agreement with published data for two Al-Cu-Mg alloys.

2. The existence of two crack growth rate transitions suggests either a change in the rate controlling kinetics or a change in the corrosion fatigue mechanism as a function of pressure. The low pressure transition may be reasonably attributed to hydrogen embrittlement. However, the frequency-insensitive high pressure transition may be due to a change of rate controlling process, a change of specific embrittlement mechanism, or the onset of some other mechanism, such as anodic dissolution, acting in concert with or instead of hydrogen embrittlement.

3. The effect of frequency on fatigue crack growth rates was insignificant under hard vacuum and over the entire range of water vapor pressures tested.

4. Corrosion fatigue of 7475-T651 in water vapor is not due to a simple interaction (superposition) of mechanical fatigue and stress corrosion cracking but is more likely the result of a more complex phenomenon.

5. Differences in the amount of residual deformation and transverse cracking on the fracture surfaces of specimens tested in water vapor and vacuum may be evidence of environmental interaction with the plastic zone ahead of the crack tip. Reduced residual deformation and transverse cracking on the fracture surfaces of specimens tested in water vapor may be the result of localized embrittlement within the plastic zone.

REFERENCES

[1] Broom, Trevor; and Nicholson, Anthony: Atmospheric Corrosion - Fatigue of Age-Hardened Aluminum Alloys. J. Inst. Metals, vol. 89, 1961, pp. 183-190.

[2] Bradshaw, F. J.; and Wheeler, C.: The Influence of Gaseous Environment and Fatigue Frequency on the Growth of Fatigue Cracks in Some Aluminum Alloys. Int. J. Frac. Mech., vol. 5, no. 4, Dec. 1969, pp. 255-268.

[3] Bradshaw, F. J.; and Wheeler, C.: The Effect of Environment on Fatigue Crack Growth in Aluminum and Some Aluminum Alloys. Appl. Matls. Res., vol. 5, April 1966, pp. 112-120.

[4] Hartman, A.: On the Effect of Oxygen and Water Vapor on the Propagation of Fatigue Cracks in 2024-T3 Alclad Sheet. Int. J. Frac. Mech., vol. 1, no. 3, Sept. 1965, pp. 167-188.

[5] Wei, R. P.: Fatigue-Crack Propagation in a High-Strength Aluminum Alloy. Int. J. Frac. Mech., vol. 4, no. 2, June 1968, pp. 159-170.

[6] Hartman, A.; Jacobs, F. A.; Nederveen, A.; and DeRijk, P.: Some Tests on the Effect of Environment on the Propagation of Fatigue Cracks in Aluminum Alloys. NLR TN M. 2182, Nat. Aerosp. Lab. (The Netherlands), 1967.

[7] Feeney, J. A.; McMillan, J. C.; and Wei, R. P.: Environmental Fatigue Crack Propagation of Aluminum Alloys at Low Stress Intensity Levels. Boeing Co. Report D6-60114, 1969.

[8] Wei, R. P.; Pao, P. S.; Hart, R. G.; Weir, T. W.; and Simmons, G. W.: Fracture Mechanics and Surface Chemistry Studies of Fatigue Crack Growth in an Aluminum Alloy. Met. Trans. A, vol. 11 A, Jan. 1980, pp. 151-158.

(9) Dicus, Dennis L.: Fatigue Crack Growth in 7475-T651 Aluminum Alloy Plate in Hard Vacuum and Water Vapor. M. S. Thesis, The George Washington University, Washington, DC, Nov. 1981.

(10) Hudson, C. Michael: A Study of Fatigue and Fracture in 7075-T6 Aluminum Alloy in Vacuum and Air Environments. NASA TN D-7262, 1973.

(11) Newman, J. C., Jr.: Crack-Opening Displacements in Center-Crack, Compact, and Crack-Line Wedge-Loaded Specimens. NASA TN D-8268, 1976.

(12) Marcus, H. L.: Gaseous Environmental Effects on Fatigue Crack Growth. Environmental Degadation of Engineering Materials, M. R. Louthan, Jr. and R. P. McNutt, eds., Virginia Tech, 1977, pp. 41-54.

(13) Marcus, H. L.: Environmental Effects II: Fatigue Crack Growth in Metals and Alloys. Fatigue and Microstructure, ASM, 1979, pp. 365-383.

(14) Weir, T. W.; Simmons, G. W.; Hart, R. G.; and Wei, R. P.: A Model for Surface Reaction and Transport Controlled Fatigue Crack Growth. Scripta Met., vol. 14, no. 3, 1980, pp. 357-364.

(15) Wei, R. P.; and Simmons, G. W.: Recent Progress in Understanding Environment Assisted Fatigue Crack Growth. Int. J. of Fracture, vol. 17, no. 2, Apri 1981, pp 235-247.

TABLE 1.- CHEMICAL COMPOSITION OF 7475 IN WEIGHT PER CENT

Zn		Mg		Cu		Cr		Fe	Si	Mn	Ti	Others		Al
Max.	Min.	Max.	Min.	Max.	Min.	Max.	Min.	Max.	Max.	Max.	Max.	Each	Total	
6.2	5.2	2.6	1.9	1.9	1.2	0.25	0.18	0.12	0.10	0.06	0.06	0.05	0.15	Bal.

TABLE 2.- TENSILE AND FRACTURE PROPERTIES OF 25.4 mm THICK 7475-7651 PLATE

Modulus of elasticity, GPa (a)		Ultimate tensile strength, MPa (a)		0.2% offset yield strength, MPa (a)		Elongation, % in 51 mm (a)		Plane strain fracture toughness, $MN/m^{3/2}$ (b)	
Long.	Trans.	Long.	Trans.	Long.	Trans.	Long.	Trans.	LT	TL
71.7	73.1	572	578	525	515	15.2	14.9	49.9	37.4

[a]Average of 5 tests

[b]One test, as reported by manufacturer

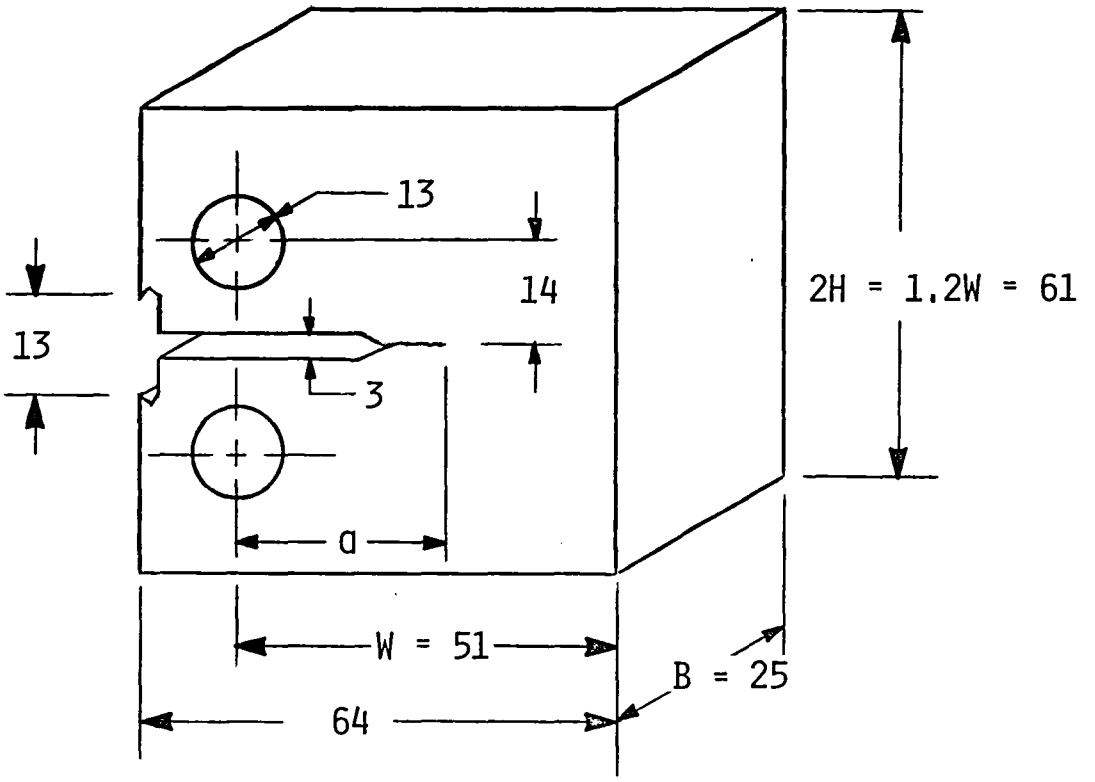

FIG. 1 - Compact specimen configuration (dimensions in mm).

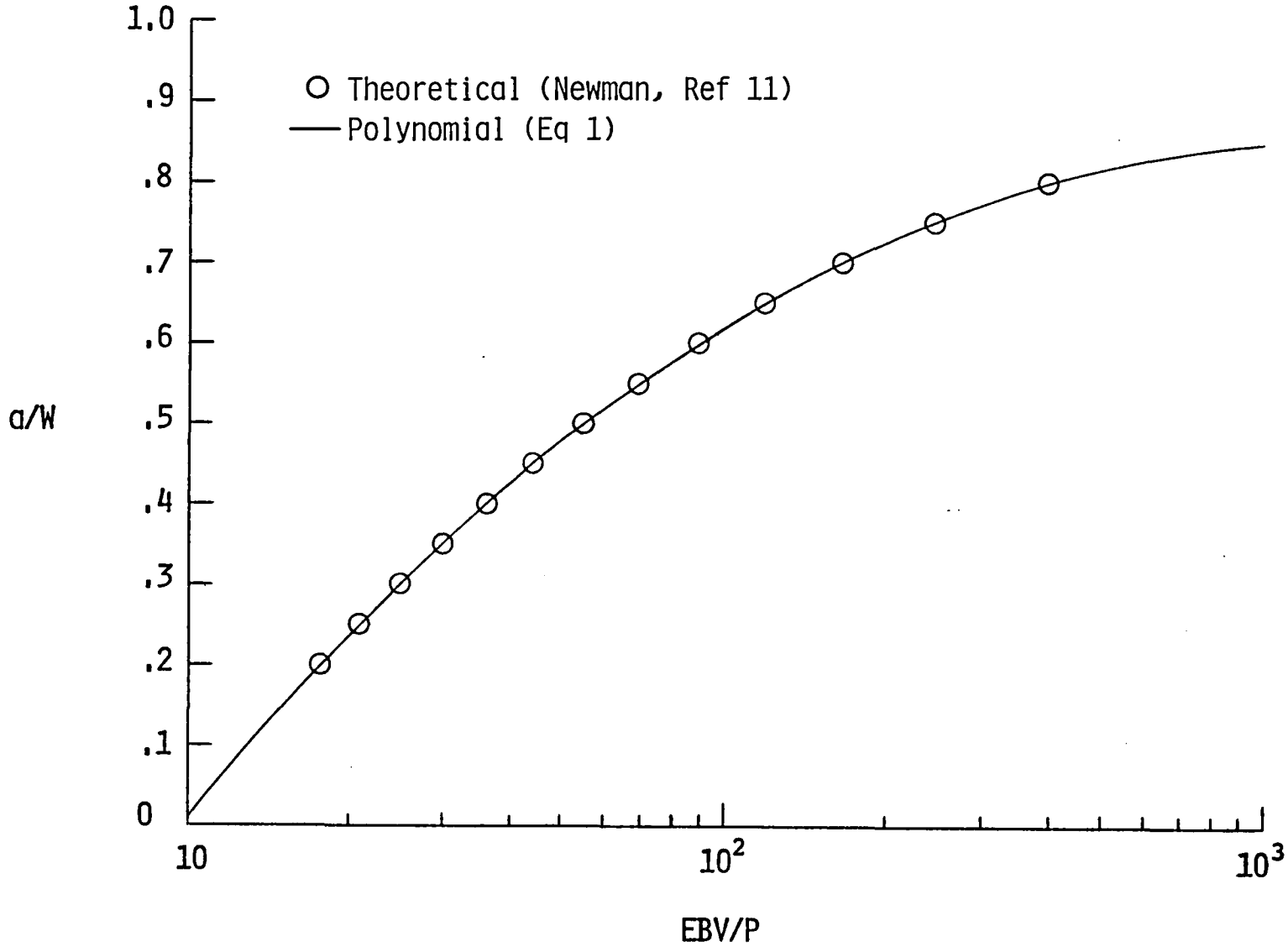

FIG. 2 - Comparison of theoretical compliance for the CT specimen configuration with a fitted polynomial.

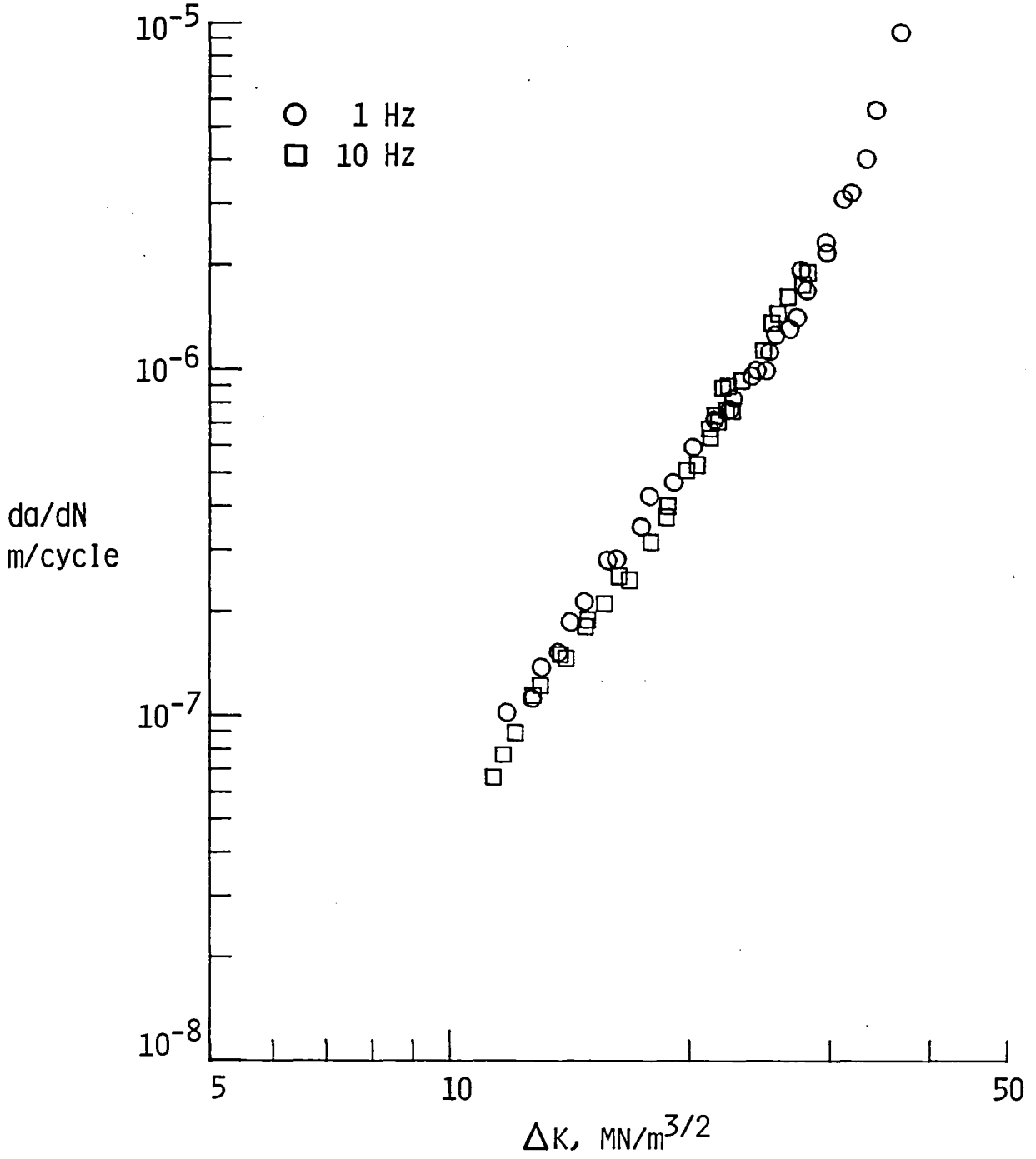

FIG. 3 - Fatigue crack growth rate in the LT orientation for 7475-T651 in a vacuum of 130 μPa at frequencies of 1 Hz and 10 Hz. R = 0.2.

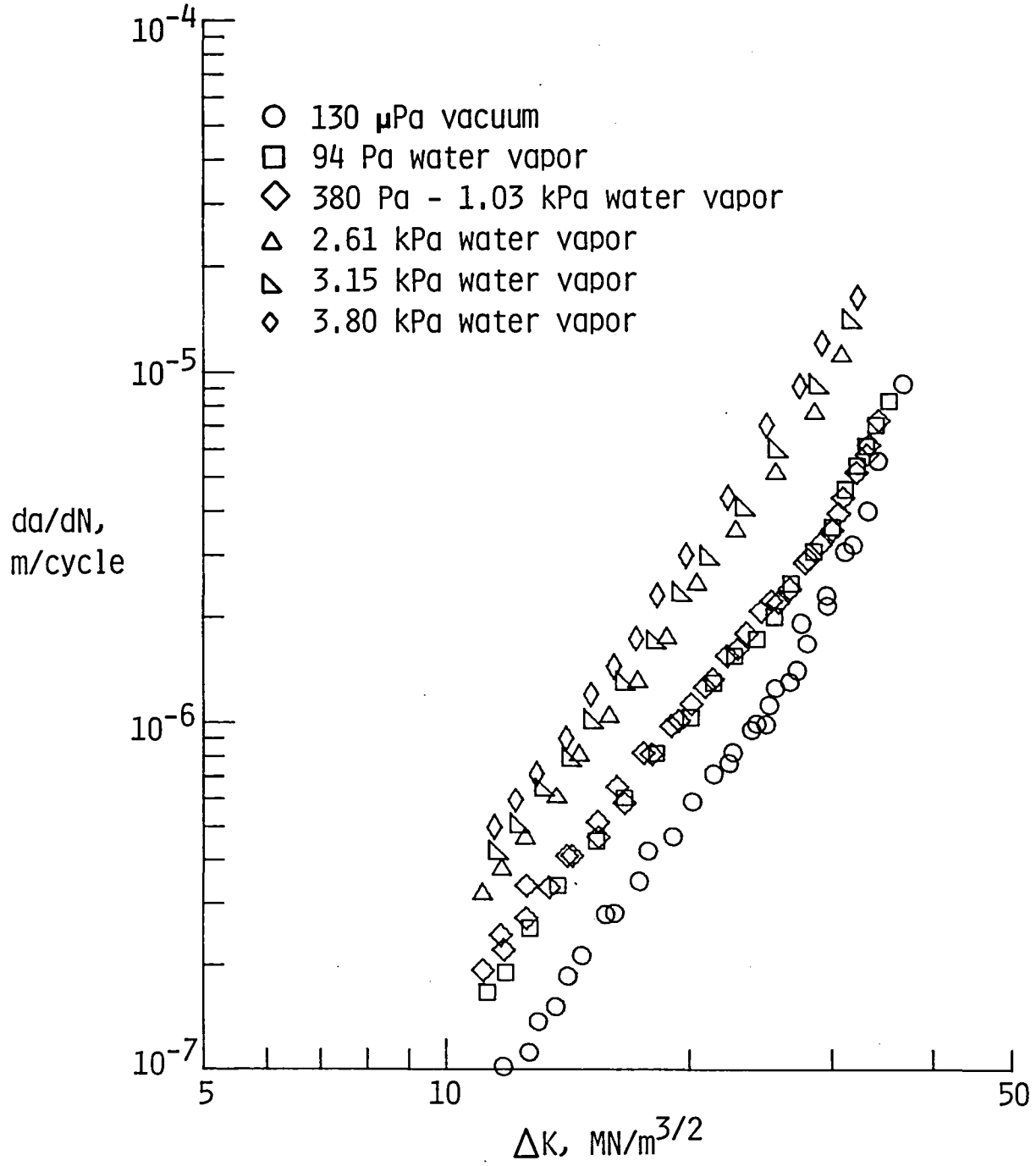

FIG. 4 - Comparison of fatigue crack growth rates for 7475-T651 at various water vapor pressures and in a vacuum of 130 μPa at a frequency of 1 Hz. LT orientation; R = 0.2.

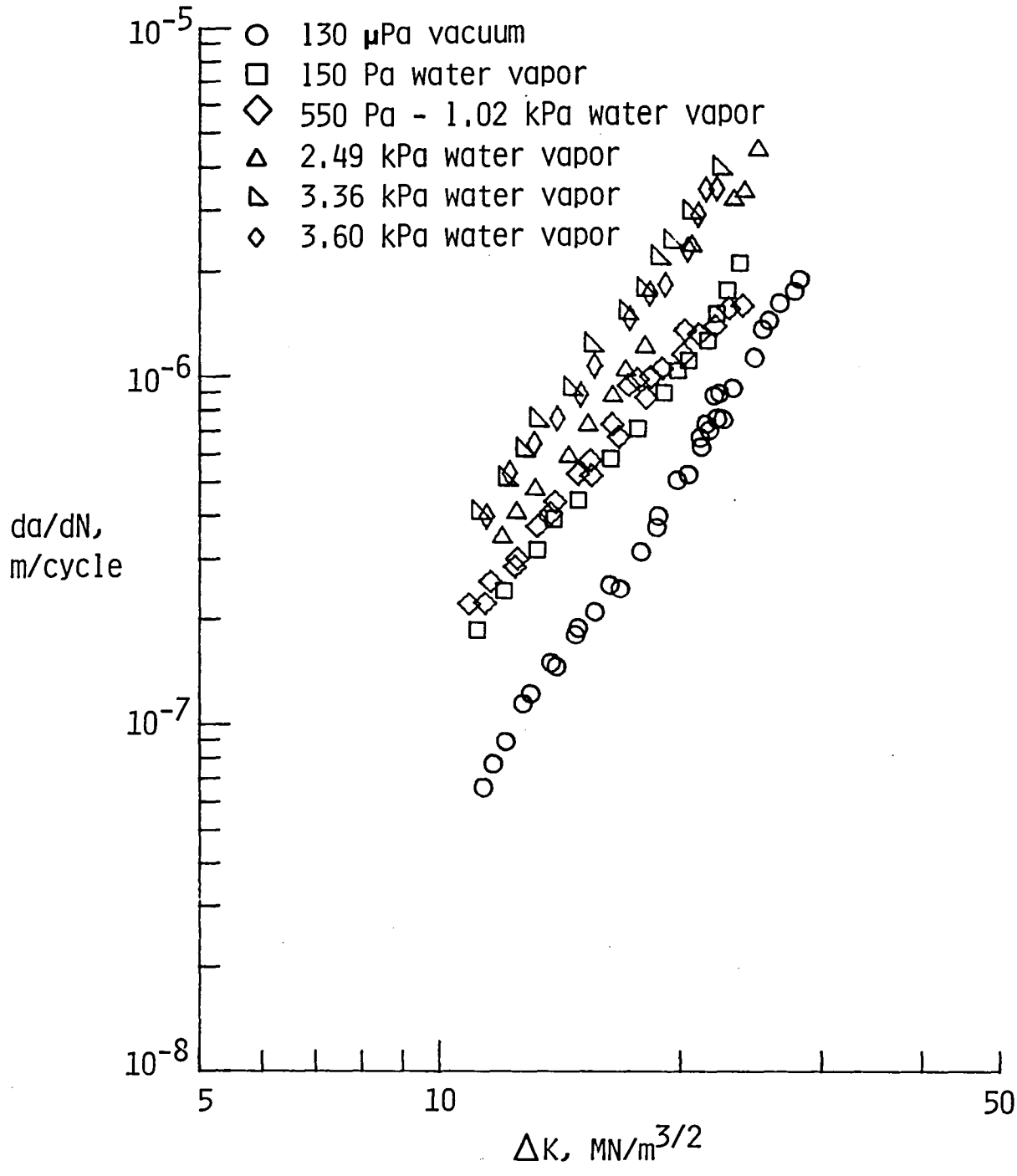

FIG. 5 - Comparison of fatigue crack growth rates for 7475-T651 at various water vapor pressures and in a vacuum of 130 µPa at a frequency of 10 Hz. LT orientation; R 0.2.

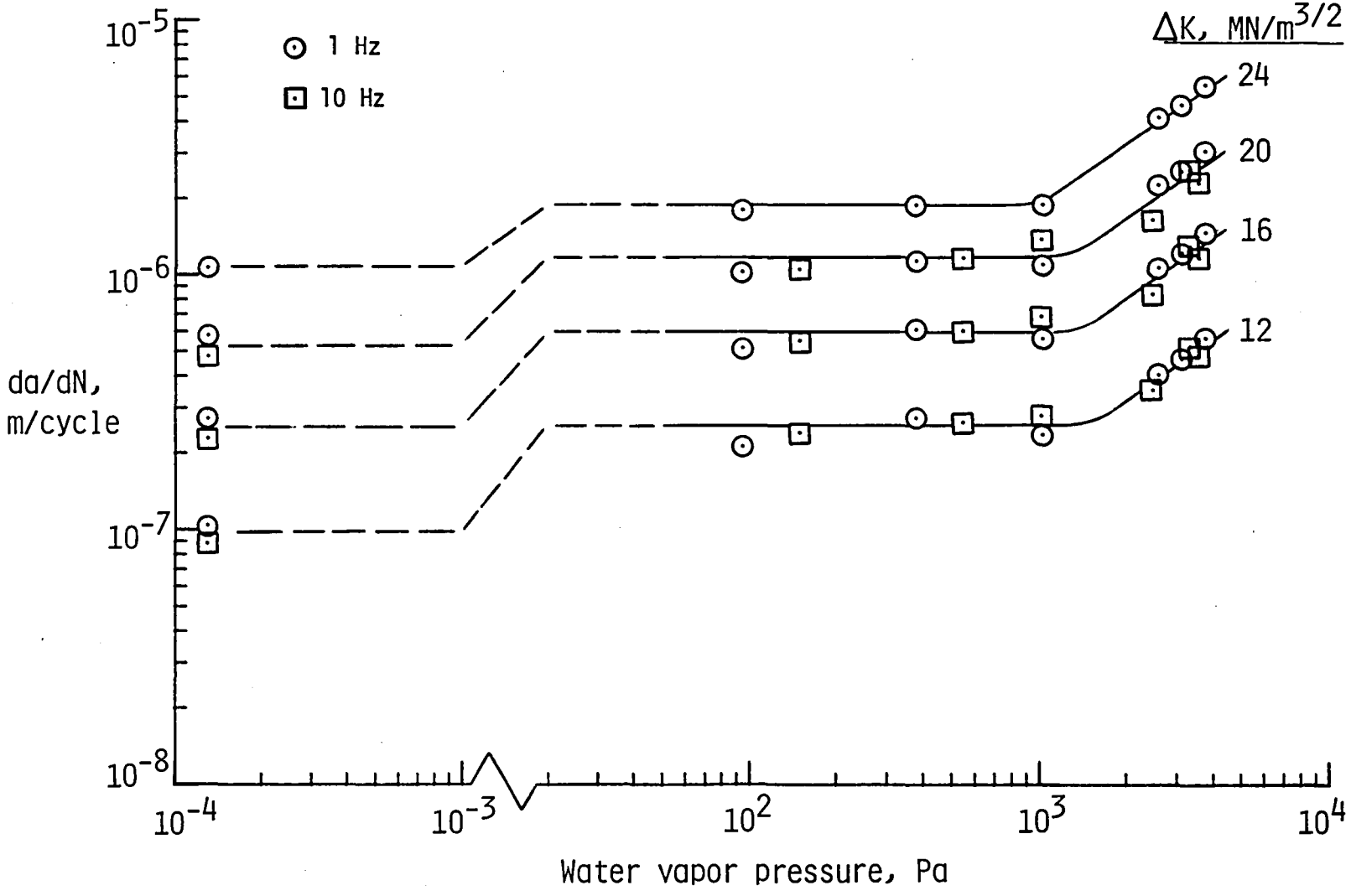

FIG. 6 - Variation of da/dN with water vapor pressure for 7475-T651 at constant ΔK values. LT orientation; R = 0.2.

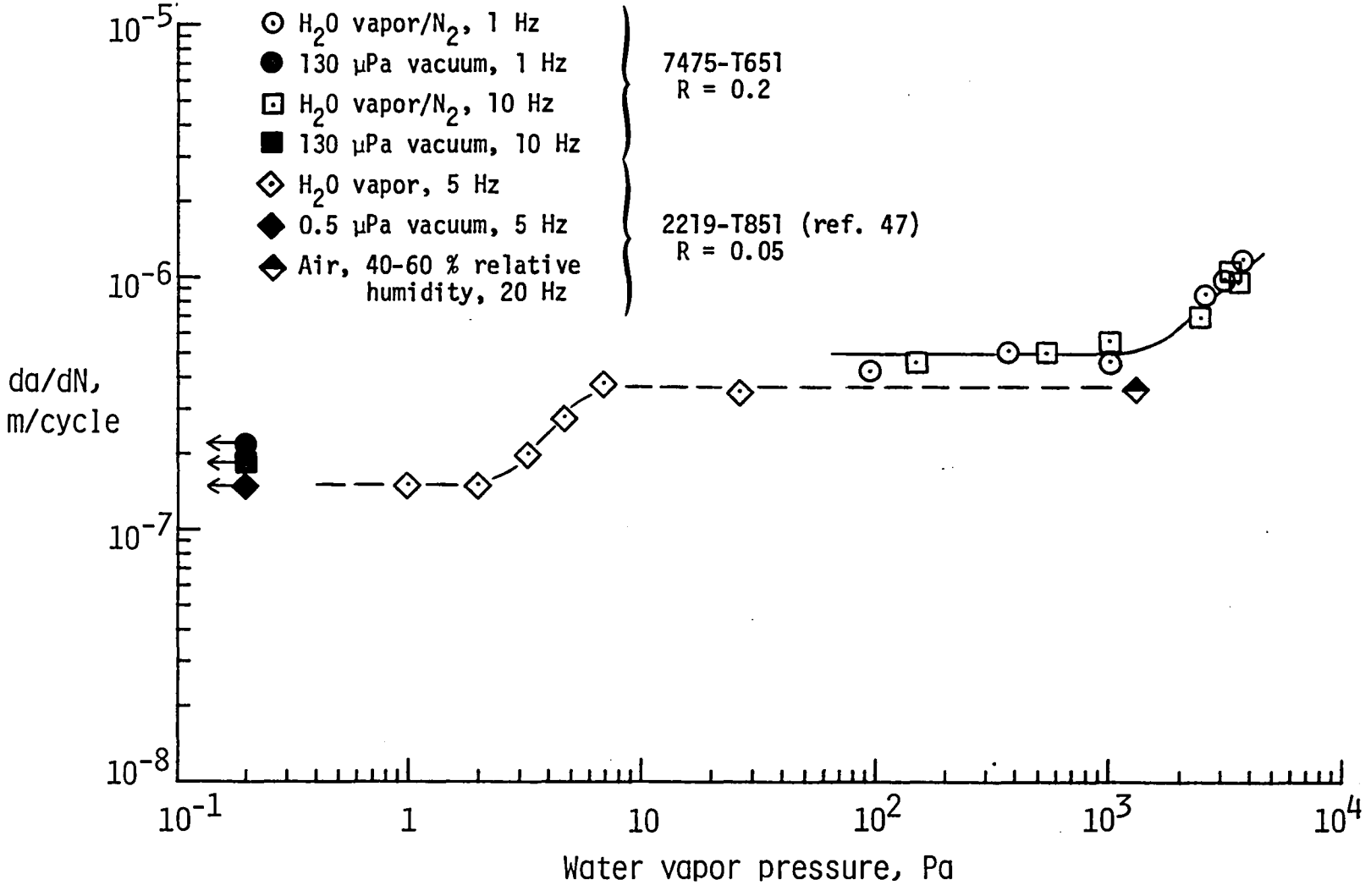

FIG. 7 - Comparison of the variation of da/dN with water vapor pressure for 7475-T651 and 2219-T851 at ΔK = 15 $MN/m^{3/2}$.

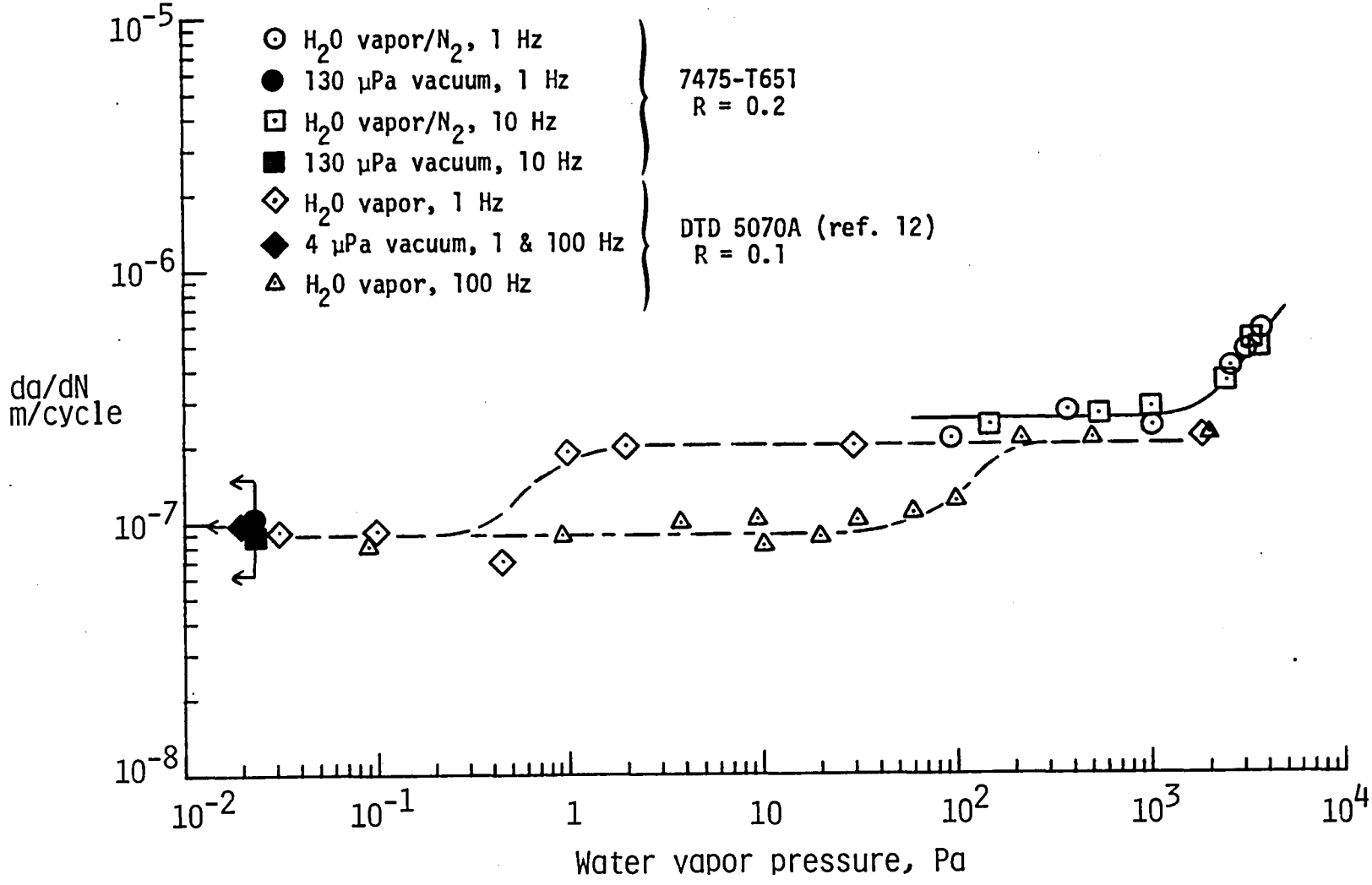

FIG. 8 - Comparison of the variation of da/dN with water vapor pressure for 7475-T651 and DTD 5070A at ΔK = 12 $MN/m^{3/2}$.

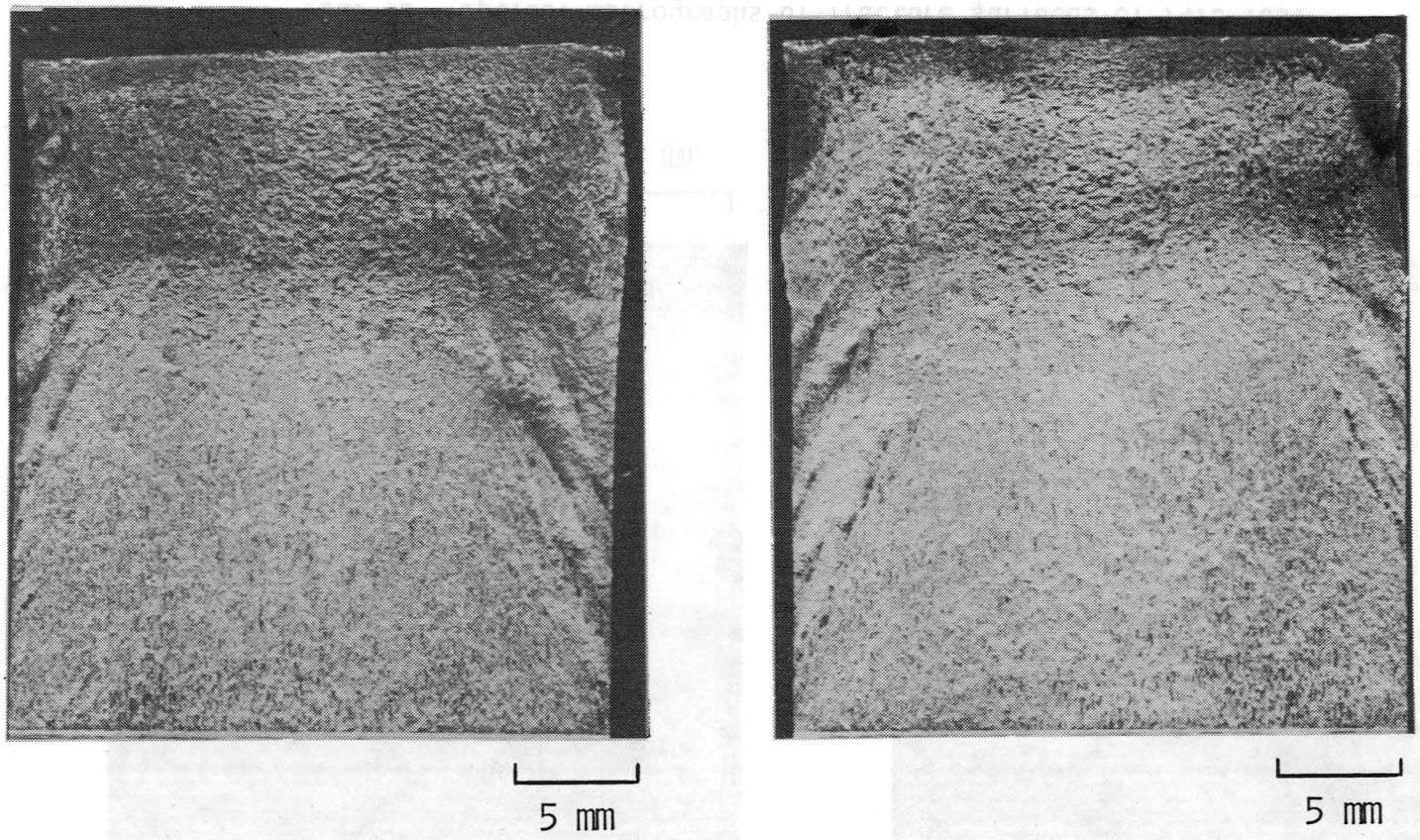

FIG. 9 - Optical macrographs of fracture surfaces of 7475-T651 specimens fatigued in vacuum.

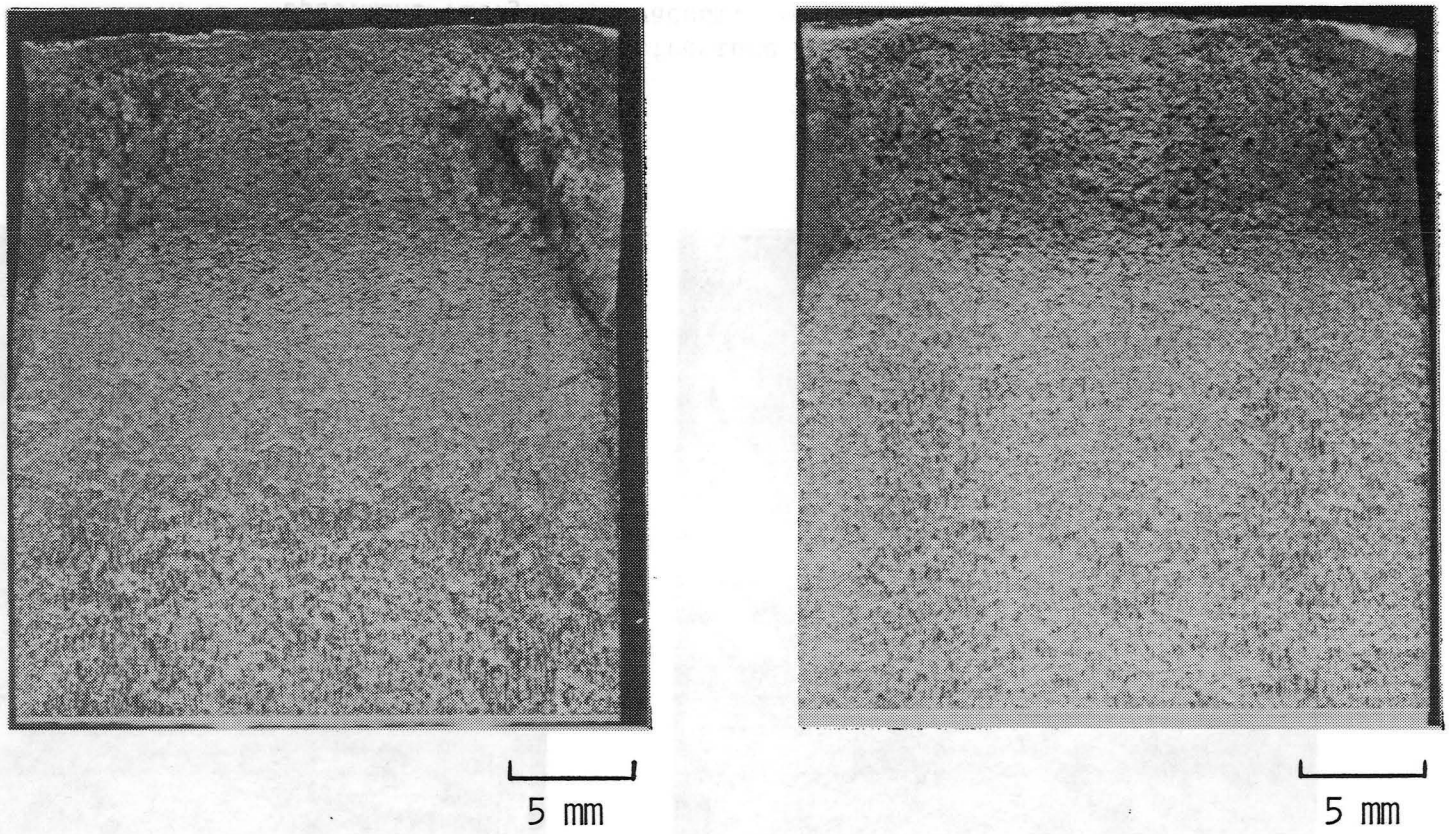

(a) 150 Pa (b) 3.6 kPa

FIG. 10 - Optical macrographs of fracture surfaces of 7475-T651 specimens fatigued at low and high water vapor pressure.

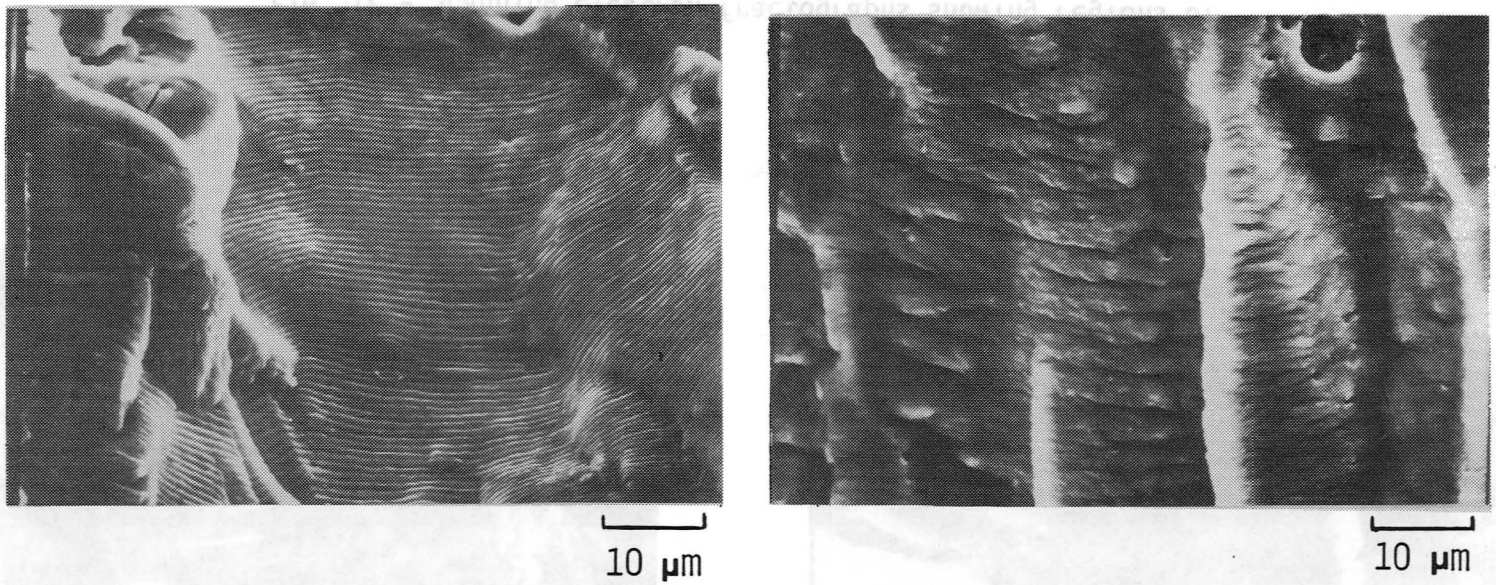

(a) 94 Pa water vapor. $\Delta K = 14\ MN/m^{3/2}$.

(b) Vacuum. $\Delta K = 15\ MN/m^{3/2}$.

FIG. 11 - Scanning electron fractorgraphs of fatigue striations formed on 7475-T651 specimens tested in water vapor and vacuum.

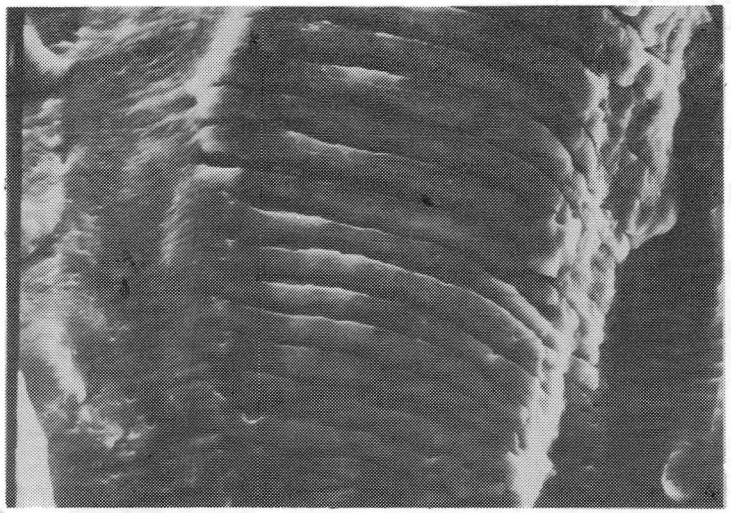

10 μm

(a) $\Delta K = 15\ MN/m^{3/2}$.

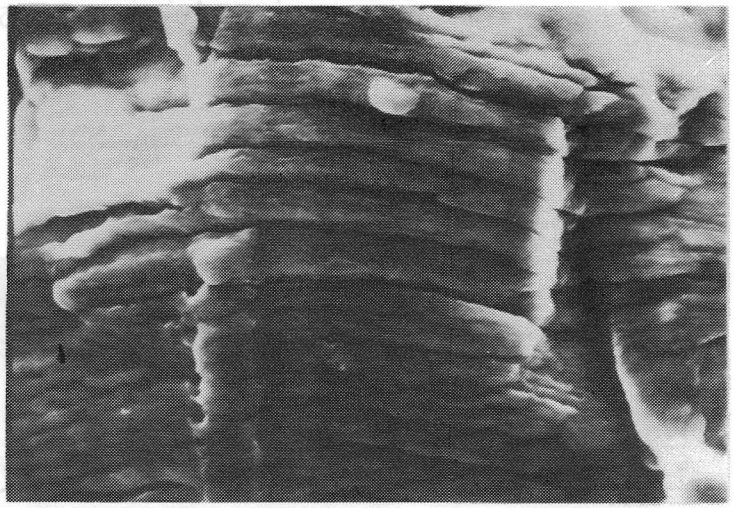

10 μm

(b) $\Delta K = 18\ MN/m^{3/2}$.

FIG. 12 - Scanning electron fractographs showing regions of transverse cracking on 7475-T651 specimens tested in vacuum.

1. Report No.	2. Government Accession No.	3. Recipient's Catalog No.
NASA TM 84477		

4. Title and Subtitle	5. Report Date
The Effect of Water Vapor on Fatigue Crack Growth in 7475-T651 Aluminum Alloy Plate	May 1982
	6. Performing Organization Code 505-33-13-01
7. Author(s)	8. Performing Organization Report No.
Dennis L. Dicus	
9. Performing Organization Name and Address	10. Work Unit No.
NASA-Langley Research Center Hampton, VA 23665	11. Contract or Grant No.
	13. Type of Report and Period Covered
12. Sponsoring Agency Name and Address	Technical Memorandum
National Aeronautics and Space Administration Washington, DC 20456	14. Sponsoring Agency Code

15. Supplementary Notes This paper was presented at an American Society for Testing and Materials sponsored Symposium on Environment-Sensitive Fracture: Evaluation and Comparison of Test Methods held at Gaithersburg, Maryland, on April 26-28, 1982 and was submitted to the Society for inclusion in a Special Technical Publication of the symposium proceedings.

16. Abstract

An investigation was performed to assess the effects of water vapor on fatigue crack growth in 7475-T651 aluminum alloy plate at frequencies of 1 Hz and 10 Hz. Twenty-five mm thick compact specimens were subjected to constant amplitude fatigue testing at a load ratio of 0.2. Fatigue crack growth rates were calculated from effective crack lengths determined using a compliance method. Tests were conducted in hard vacuum and at water vapor partial pressures ranging from 94 Pa to 3.8 kPa.

Fatigue crack growth rates were frequency-insensitive under all environmental conditions tested. For constant stress intensity factor ranges crack growth rate transitions occurred at low and high water vapor pressures. Crack growth rates at intermediate pressures were relatively constant and showed reasonable agreement with published data for two Al-Cu-Mg alloys. The existence of two crack growth rate transitions suggests either a change in rate controlling kinetics or a change in corrosion fatigue mechanism as a function of water vapor pressure. Reduced residual deformation and transverse cracking specimens tested in water vapor versus vacuum may be evidence of embrittlement within the plastic zone due to environmental interaction.

17. Key Words (Suggested by Author(s))	18. Distribution Statement
aluminum alloy, compliance, corrosion fatigue, fatigue crack growth rate, fractography, frequencies, vacuum, water vapor	Unclassified-Unlimited Subject Category 26

19. Security Classif. (of this report)	20. Security Classif. (of this page)	21. No. of Pages	22. Price
Unclassified	Unclassified	34	A03

For sale by the National Technical Information Service, Springfield, Virginia 22161